Chinese Chemical Letters 32 (2021) 3066–3070

Contents lists available at ScienceDirect

Chinese Chemical Letters

journal homepage: www.elsevier.com/locate/cclet

Communication

Molecular engineering and biomedical applications of ultra-sensitive fluorescent probe for Ag^+

Jianfei Kan[a,1], Xiaonan Zhou[a,1], Yanyan Sun[a], Liyuan Sun[a], Hao Chu[a], Zhaosheng Qian[b,*], Jin Zhou[a,*]

[a] School of Pharmacy, Maternal and Child Health Hospital of Weifang Medical University, Weifang Medical University, Weifang 261053, China
[b] College of Chemistry and Life Sciences, Zhejiang Normal University, Jinhua 321004, China

ARTICLE INFO

Article history:
Received 22 February 2021
Received in revised form 29 March 2021
Accepted 30 March 2021
Available online 31 March 2021

Keywords:
Fluorescent probe
Ag^+
Detection
Imaging
Theoretical calculation
Cell typing
Spirolactam

ABSTRACT

A series of probes **KJ-x** (**x** = **1**–**3**) with carbon chains of different lengths based on the matrix of rhodamine B were engineered to detect Ag^+ in aqueous solution in this work. Among them, **KJ-1** is selected as the best option after *in vitro* investigation in view of its most sensitive and rapid response to Ag^+, whose possible sensing mechanism is studied by experimental investigation and theoretical calculation. To identify the practical application of the probe, the detection of Ag^+ in nonantibiotic fungicide Silver&Health and differentiation between normal hepatocytes and hepatoma cells using confocal imaging was conducted.

Noble metal silver (Ag) and its derivatives play a significant part in the long history and modern civilization development of human beings [1]. For most people, Ag is known in real life for its rarity and attractive surface gloss appearance, which is fit for the production of jewellery, coins and silverware [2–4]. Owing to its germicidal characteristic of inactivating microorganisms such as gram-positive bacteria, gram-negative bacteria and fungi, Ag ions are also used as antibacterial drug for dental, vaginal or nasal sterilization and disinfection [5–7]. In recent years, Ag is more and more widely used in biomedicine, drug delivery systems and biosensors [8–11]. On the other hand, its abuse especially industrial waste from the electronic and photographic imaging industry would cause a potential threat to human health because it could inactivate sulfhydryl enzymes and combine with imidazole, amine and carboxyl groups of a wide range of metabolites, and replace Ca^{2+} and Zn^{2+} in hydroxyapatite which is an essential part of bone [12–15]. As a result, the excessive Ag would lead to the occurrence of various diseases such as growth retardation, anemia, heart enlargement, neurodegenerative diseases, and insoluble sediments induced damage on skin, kidney and cornea [16–19]. Thus, the development of a rapid, selective and sensitive method for the detection of Ag^+ has drawn intense interest, which would further reveal its physiological function and is of considerable importance for human health.

Conventional methods, such as atomic absorption or emission spectroscopy, inductively coupled plasma mass spectrometry and anodic stripping voltammetry, can be used to monitor trace levels of silver ions, but they require complex and time-consuming pretreatment and expensive apparatus [20–22]. Fluorescent probe is a simple, fast, highly sensitive and low cost method, which has real-time imaging ability to track and detect ions in biological systems in real time [23–31]. Many quantum dots based fluorescent probes have been developed for detection of silver ions in water, food or *in vivo* [32–37], but most of the probes work with relatively long response times and turn-on response type, and are susceptible to interference from other heavy metal ions such as Hg^{2+}, Cu^{2+} or Fe^{3+}, which are not fit for the selective, sensitive and rapid sensing. The development of fluorescent probes based on small molecules may provide the new option to solve the above issues.

To this end, a series of probes **KJ-x** (**x** = **1**–**3**) (Scheme 1) with carbon chains of different lengths on the matrix of rhodamine B were designed and synthesized to detect Ag^+ in aqueous solution in this work. Among them, **KJ-1** is selected as the best option after *in*

* Corresponding authors.
E-mail addresses: qianzhaosheng@zjnu.cn (Z. Qian), zhoujin@wfmc.edu.cn (J. Zhou).
[1] These authors contributed to this work equally.

https://doi.org/10.1016/j.cclet.2021.03.076

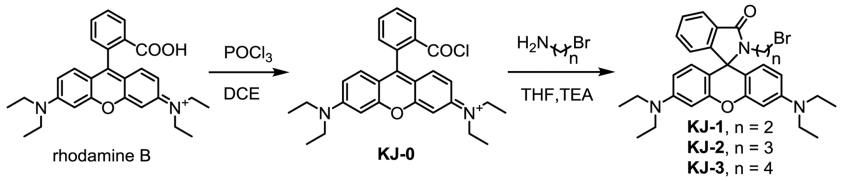

Scheme 1. Synthesis of **KJ-x**.

vitro investigation in view of its most sensitive and rapid response to Ag^+, whose possible sensing mechanism is studied by experimental investigation and theoretical calculation. To identify the practical application of the probe, the detection of Ag^+ in nonantibiotic fungicide Silver&Health (an active silver ion antibacterial solution, used for the treatment of acute rhinitis, sinusitis, acute pharyngitis and oral ulcer) and differentiation between normal hepatocytes and hepatoma cells using confocal imaging were conducted.

As shown in Scheme 1, to prepare the desired compounds, rhodamine B acyl chloride intermediate **KJ-0** was synthesized first and then reacted with bromoalkylamine of different carbon chain lengths. The resulting probe structure was well characterized by ^1H and ^{13}C NMR and high-resolution mass spectra (Figs. S1–S9 in Supporting information), and the formation of probes was demonstrated.

The response of **KJ-1** towards Ag^+ in aqueous solution (pH 7.4) was tested first after 30 min reaction. As shown in Fig. 1A, **KJ-1** itself has almost no absorption (less than 0.003) around 555 nm. Upon the addition of Ag^+ (20 μmol/L), the maximum absorption peak changes a little at wavelength (to 558 nm) while increases nearly 20 fold at intensity. Consequently, Ag^+ caused an obvious color change from almost colorless and transparent to visible pink under the daylight. As shown by the corresponding fluorescence spectra in Fig. 1B, the fluorescence signal increases sharply with a 25 fold, which is visually reflected by the right red fluorescence photograph in the inset. Encouraged by the preliminary experimental exploration, we tried to explore the structure-activity relationship of silver ion reaction with a series of homologous probes (**KJ-1**, **KJ-2** and **KJ-3**) in which there are 2, 3 and 4 saturated carbons between halogen atom bromine and nitrogen on spiro amide ring. We tested the fluorescence response of the probes towards 0, 10 and 30 μmol/L Ag^+ as time went by. The performance is shown in Fig. S10 (Supporting information), where it is noted that the reaction between 2 carbons contained **KJ-1** and Ag^+ of different concentrations could reach equilibrium almost instantaneously and the probe itself kept steady under the 60 min detection. While it takes much more time for **KJ-2** and **KJ-3** to achieve the reaction balance under the same test conditions. In addition, as the increase of carbon chain length, the obtained fluorescence after reaction becomes weaker and weaker, and the two probes themselves would fluoresce as time flies, which indicates their poor stability under physiological conditions. Based on the above results, **KJ-1** was selected as the best candidate in the next test.

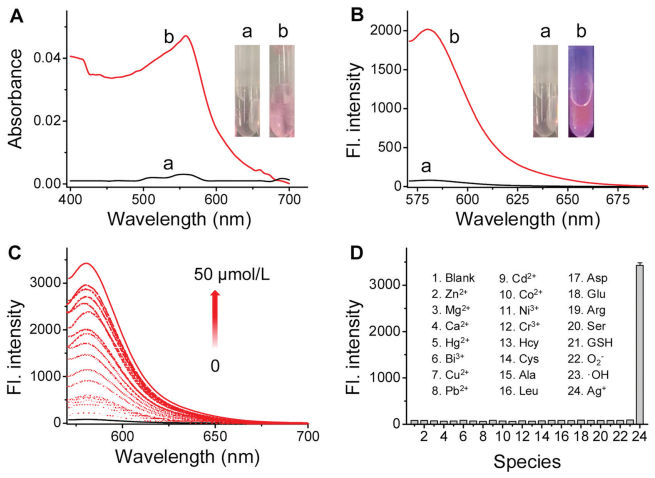

Fig. 1. (A) Absorption spectra of **KJ-1** (10 μmol/L) before (a) and after (b) reaction with Ag^+ (20 μmol/L); the inset shows the solution color changes under visible color. (B) Corresponding fluorescence spectra (λ_{ex} = 558 nm) of (A); the inset herein illustrate the color changes under 365 nm light. (C) Fluorescence spectra of **KJ-1** (10 μmol/L) reacting with Ag^+ at varied concentrations. (D) Fluorescence responses of **KJ-1** (10 μmol/L) to various substances (5 equiv.). The results are the mean ± standard deviation of three separate measurements. $\lambda_{ex/em}$ = 558/580 nm.

The study of pH and temperature on the fluorescence intensity of probe **KJ-1** in presence of Ag^+ suggests that the probe could work efficiently under the physiological conditions (Figs. S11A and B in Supporting information). Under the optimal conditions, the fluorescence spectra intensity of probe **KJ-1** increased gradually with the addition of Ag^+ from 0 to 50 μmol/L (Fig. 1C, Fig. S11C in Supporting information). The detection limit was calculated to be as low as 2.1 nmol/L based on 3σ/S (where σ is the standard deviation of the only probe contained solution and S is the slope of the sensitive calibration curve ranging from 6 nmol/L to 100 nmol/L). In order to examine the selectivity of **KJ-1**, other heavy metal ions (Hg^{2+}, Bi^{3+}, Cu^{2+}, Pb^{2+}, Cd^{2+}, Co^{2+}, Ni^{2+}, Cr^{3+}, 5.0 equiv.) and biologically representative relevant substances (Zn^{2+}, Mg^{2+}, Ca^{2+}, Hcy, Cys, Ala, Leu, Asp, Glu, Arg, Ser, GSH, O_2^-, $^{\bullet}OH$) were gauged (Fig. 1D). The results demonstrate that none of them led to a significant fluorescence enhancement except for Ag^+, suggesting its excellent selectivity.

As for the response mechanism, we proposed that probe **KJ-1** would be converted to be rhodamine derivative with oxazoline structure after the binding of Ag^+ to the bromine, which promotes the spirolactam ring opening and the production of oxazoline Rh-O, which was verified by the high resolution electrospray ionization mass spectra (HRMS, Fig. S12 in Supporting information). We also studied the spectroscopic difference with rhodamine B (RD-B). The maximum absorption peak of Ag^+ added **KJ-1** solution is very near to that of the RD-B solution (Fig. S13A in Supporting information). However, there is a noticeable fluorescence emission difference between them. The emission peak locates at 575 nm, where there is a 5 nm decrease compared to that of the product Rh-O after probe **KJ-1** reaction, further suggesting that the product is not RD-B (Fig. S13B in Supporting information). To further understand the reaction mechanism and the difference of three probes in response to silver ion, DFT calculations were performed. As shown in Fig. 2A, it is proposed that two elementary reactions are involved in the response mechanism. In the first elementary reaction, a SN_2 substitution reaction takes place first to form the cyclized structure and the bromine atom is transformed to the negative bromide ion, which forms a transient intermediate with no charge. Then, the silver ion binds with negative bromide ion to produce AgBr precipitate in the secondary reaction, and such a precipitation greatly promotes the whole forward reaction. The energy differences between reactant, intermediate and product for

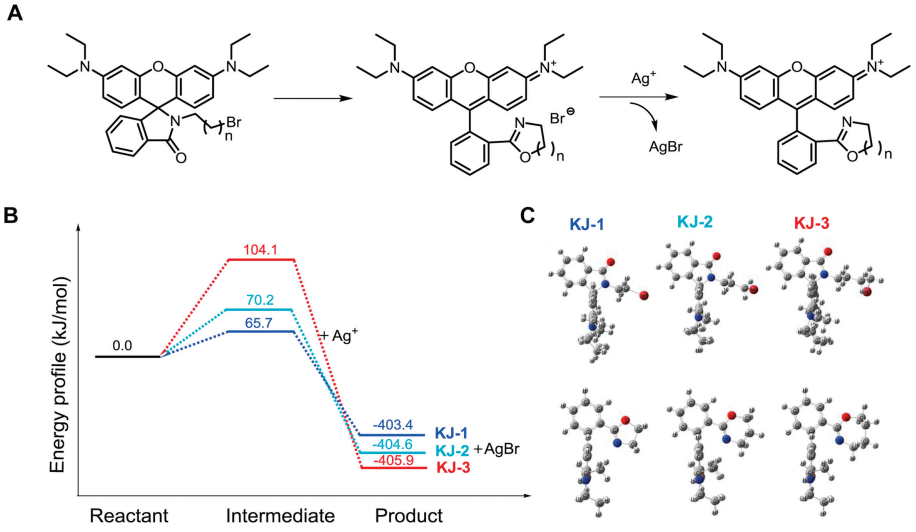

Fig. 2. (A) Response mechanism. Energy profiles of the proposed reaction route (B) and optimized structures (C).

KJ-1, **KJ-2** and **KJ-3** were calculated with DFT calculations. Fig. 2B shows that the all the energy gaps are positive for the first step, suggesting these reactions are unflavored thermodynamically. All calculated values for the second step of three probes are negative and no much difference exists among them, indicating that the second reaction is much favored thermodynamically and the precipitation reaction plays a key role to promote the whole reaction. But the energy gap for **KJ-1** is the lowest in the first step among these three probes, clearly indicating that the reaction starting from **KJ-1** is more favorable than that of the others because the first step is the rate-determining step, which sufficiently supports the experimental observations that all three probes can respond to Ag^+ but only **KJ-1** has the best response to silver ion. The optimized structures of reactants and products for **KJ-1**, **KJ-2** and **KJ-3** are shown in Fig. 2C, where it is clearly observed that a cyclization reaction occurs accompanying the change of bromine to bromide ion during the substitution reaction. These conclusions are also consistent with common knowledge that the formation of five-member ring is most favorable thermodynamically, and well supports our experimental observations.

The accuracy of the detection results directly affects the future application potential of the probe. Next, Ag^+ was determined in commercial nonantibiotic fungicide Silver&Health to explore the practical application of this method using a standard addition method. The estimated recoveries (between 94% and 106%) and the relative standard derivation (RSD, less than 2%, $n = 3$) are listed in Table 1 by adding Ag^+ of different concentrations into spiked Silver&Health solution. Ideal recoveries and low RSD were obtained for spiking experiments, which indicate that the developed **KJ-1** can be employed reliably to detect Ag^+ with great potential.

In view of the above excellent performance for sensing Ag^+, we next further delved into the application of **KJ-1** in biological system. The performance of cytotoxicity test in living BEL-7402 cells (human hepatoma cells) *via* MTT assay showed that the cell viability of **KJ-1** was more than 82% when its concentration is as high as 50 μmol/L, as shown in Fig. S14 (Supporting information), suggesting its low cytotoxicity and good biocompatibility. It is widely known that the Cl^- at physiological concentration (mmol/L level) is prone to cause the precipitation of Ag^+, which might compete with probe reaction. To get rid of this concern, we further carried out an *in vitro* experiment to study the influence of added anion Cl^- with considerable concentration (mmol/L level) at pH 7.4 PBS solution. As shown in Fig. S15 (Supporting information), Cl^- with high physiological concentration (from 1 mmol/L to 5 mmol/L) causes slight fluorescence decline, which ensures that the probe can still work effectively in the cells. Subsequently, the laser confocal fluorescent imaging of probe **KJ-1** was carried out. The time dependence for probe in fluorescence imaging showed that the probe could enter the cells efficiently and quickly and the probe incubation time of 20 min could achieve the reaction equilibrium time when the concentration of Ag^+ is a constant (Fig. S16 in Supporting information). In the actual test process, in order to ensure full response, 30 min is adopted. Then the time dependence for Ag^+ is studied. As depicted in Fig. 3A, almost no fluorescence could be observed in BEL-7402 cells only treated with probe **KJ-1**. After BEL-7402 cells had been pretreated with Ag^+, the noticeable fluorescence signals could be observed and the signal intensity increased gradually when the concentration of added Ag^+ grew from 1 μmol/L to 20 μmol/L. To further confirm the Ag^+ induced fluorescence response to **KJ-1**, a classical chelating ligand ethylene diamine tetraacetic acid (EDTA) was added into the culture medium prior to the before the two reactants **KJ-1** and Ag^+ came into contact. As shown in Figs. 3A-f, EDTA showed an effective masking effect for Ag^+. This phenomenon is consistent with the changing trend reflected by flow cytometry which is a high-throughput detection method (Fig. 3B). Then we carried out the practical application in Silver&Health imaging in Fig. S17 (Supporting information). The drug Silver&Health rich in Ag^+ could also cause an impressive fluorescence enhancement no matter in the confocal imaging or flow cytometry.

Now that **KJ-1** is able to sense the Ag^+ fluctuation induced either by a standard Ag^+ direct addition or Ag^+ contained drug in cancer cell BEL-7402 in the above study, it would be of great interest to tell the difference between the homologous cancer cells and normal cells from the same species and reveal the potential mechanism behind it. We might as well choose two cells from human liver, cancer cells (BEL-7402) and normal cells (L-02), as the experimental subjects to observe the fluorescence changes under the same

Table 1
Detection of Ag^+ in Silver&Health (1×10^5-fold diluted).

Ag^+ added (nmol/L)	Ag^+ found (nmol/L)	Recovery (%)	RSD (%)
0	18.6	–	–
10	28.01 ± 0.19	94.24	1.94
30	50.28 ± 0.52	105.64	1.72
50	69.32 ± 0.39	101.47	0.78

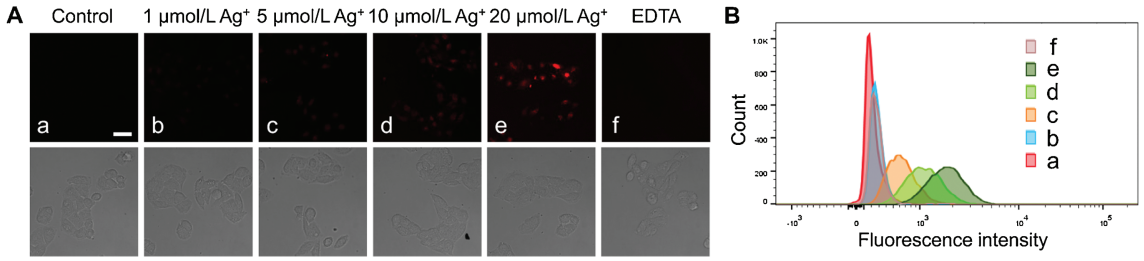

Fig. 3. (A) Laser confocal fluorescence microscopic images of BEL-7402 cells under different conditons. (a) Only **KJ-1** (10 μmol/L) 30 min treatment; (b-e) Pretreatment with 1 μmol/L, 5 μmol/L, 10 μmol/L and 20 μmol/L Ag^+ respectively for 30 min, then cultured with **KJ-1** (10 μmol/L) contained medium for 30 min; (f) Pretreatment with 20 μmol/L Ag^+ first for 30 min, then 20 μmol/L EDTA was added prior to the **KJ-1** (10 μmol/L) culture for 30 min. The directly below the dark field are corresponding DIC images; scale bar: 30 μm; λ_{ex} = 560 nm, λ_{em} = 570–650 nm. (B) Flow cytometric analysis of above respective cells.

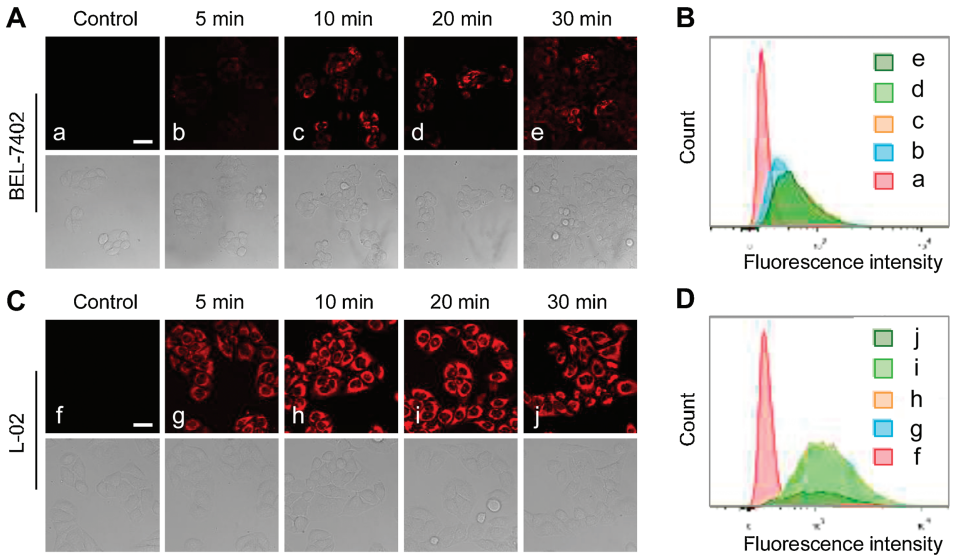

Fig. 4. Comparation of confocal fluorescence microscopic images between BEL-7402 cells and L-02 cells under different treatment time of Ag^+. (A) BEL-7402 cells were treated with medium containing probe (10 μmol/L) for 30 min, then $AgNO_3$ solution (10 μmol/L) at 37 °C for 5 min, 10 min, 20 min, and 30 min repectively before imaging. (C) L-02 cells were treated as those in (A). The directly below the dark field are corresponding DIC images; scale bar: 30 μm; λ_{ex} =560 nm, λ_{em} = 570–650 nm. (B) and (D) are corresponding flow cytometric analysis data of (A) and (C) respectively.

experimental conditions. Both cells were divided into 5 groups and incubated with 10 μmol/L Ag^+ for 0 (control group), 5, 10, 20 and 30 min respectively before the **KJ-1** incubation. From Figs. 4A and C, we can intuitively see that in the initial stage of reaction time (5 min), the fluorescence signal for BEL-7402 cells is much weaker than that for L-02 cells. In the meanwhile, compared to the L-02 cells, even in the same kind of cells BEL-7402, the initial signal intensity is much lower than that when the reaction reaches equilibrium. Moreover, it is noted that the intensity of BEL-7402 cells is inferior to the signal from the L-02 cells when both kinds of cells are in the state of reaction equilibrium. The flow cytometry analysis was performed to further evaluate the difference of these changes, as shown in Figs. 4B and D, which solidly support the trend of fluorescence intensity in terms of more quantity. Considering the differences in physiology and pathology for the two kinds of cells, the greater signal intensity may be due to the richer intracellular mercapto proteins in the cancer cells, which is prone to bond the added Ag^+ and causes the probe produce the weak fluorescence. We infer that this effect is more evident in the beginning in the cancer cells because the limited silver ions are effectively adsorbed by sulfhydryl proteins. As the incubation time is extended, more Ag^+ would enter the cancer cells which overflows the masking ability of intracellular mercapto proteins. Therefore, these results suggest that probe **KJ-1** is able to indicate the difference between the difference between the homologous cancer cells and normal cells.

In conclusion, a rapid fluorescent probe, **KJ-1**, was constructed to selectively and sensitively detect Ag^+ in nonantibiotic fungicide in a turn-on type fluorescent response. The possible response mechanism based on tandem spiro amide ring opening and the formation of new ring triggered by Ag^+ to the bromine of the probe is studied by experimental investigation and theoretical calculation. Also, this probe was successfully applied to distinguish homologous cancer cells and normal cells. The present protocol supplies a new pathway for the test of silver related consumer product and disease diagnosis.

Declaration of competing interest

The authors report no declarations of interest.

Acknowledgments

We are grateful for the financial support from the National Natural Science Foundation of China (No. 21705120), the Project of Shandong Province Higher Educational Outstanding Youth Innovation Team (No. 2019KJM008), the Natural Science Foundation of Shandong Province, China (No. ZR2017LB016), the Project of

Shandong Province Higher Educational Science and Technology Program (No. J17KB074).

Appendix A. Supplementary data

Supplementary material related to this article can be found, in the online version, at doi:https://doi.org/10.1016/j.cclet.2021.03.076.

References

[1] M. She, Z. Wang, J. Chen, et al., J. Sci. Commun. 432 (2021) 213712.
[2] S. Singha, D. Kim, H. Seo, S.W. Cho, K.H. Ahn, Chem. Soc. Rev. 44 (2015) 4367–4399.
[3] X. Zhang, S. Chen, S. Jin, et al., Sens. Actuators B: Chem. 237 (2016) 367–372.
[4] H. Wu, J. Jia, Y. Xu, X. Qian, W. Zhu, Sens. Actuators B: Chem. 265 (2018) 59–66.
[5] S. Jiang, Y. Zhang, Y. Yang, et al., ACS Appl. Mater. Interfaces 11 (2019) 10554–10558.
[6] X.B. Zhang, Z.X. Han, Z.H. Fang, G.L. Shen, R.Q. Yu, Anal. Chim. Acta 562 (2006) 210–215.
[7] J. Sun, J. Yue, P. Wang, H. He, Y. Jin, J. Mater. Chem. C 1 (2013) 908–913.
[8] F. Wang, R. Nandhakumar, J.H. Moon, et al., Inorg. Chem. 50 (2011) 2240–2245.
[9] J.F. Zhang, Y. Zhou, J. Yoon, et al., Chem. Soc. Rev. 40 (2011) 3416–3429.
[10] A. Chatterjee, M. Santra, N. Won, et al., J. Am. Chem. Soc. 131 (2009) 2040–2041.
[11] Z. Chen, H. Zhou, W. Gu, et al., J. Photochem. Photobiol. A 379 (2019) 5–10.
[12] W. Zhang, Y. Luo, Y. Zhang, et al., Dye. Pigments 176 (2020) 108235.
[13] K.B. Holt, A.J. Bard, Biochemistry 44 (2005) 13214–13223.
[14] P. Thamaraiselvi, N. Duraipandy, M.S. Kiran, et al., ACS Sustain. Chem. Eng. 7 (2019) 9865–9874.
[15] Y. Zhang, W. Chen, X. Dong, et al., Sens. Actuators B: Chem. 261 (2018) 58–65.
[16] B.H. Kang, Z.F. Gao, Na. Li, et al., Talanta 156–157 (2016) 141–146.
[17] H.Y. Tang, Y. Gao, B. Li, C.W. Li, Y. Gao, Sens. Actuators B: Chem. 270 (2018) 562–569.
[18] W. Shen, L. Wang, M. Wu, X. Bao, Inorg. Chem. Commun. 70 (2016) 107–110.
[19] K.S. Hwang, K.Y. Park, D.B. Kim, S.K. Chang, Dye. Pigments 147 (2017) 413–419.
[20] W. Saiyasombat, S. Kiatisevi, RSC Adv. 11 (2021) 3703–3712.
[21] M. Li, H. Gou, I. Al-Ogaidi, N. Wu, ACS Sustain. Chem. Eng. 1 (2013) 713–723.
[22] F. Ye, X.M. Liang, K.X. Xu, et al., Talanta 200 (2019) 494–502.
[23] L. Huang, Y. Chen, Y. Zhao, et al., Chin. Chem. Lett. 31 (2020) 2941–2944.
[24] N. Zhou, F. Huo, Y. Yue, et al., Chin. Chem. Lett. 31 (2020) 2970–2974.
[25] P. Lu, X. Zhang, T. Ren, et al., Chin. Chem. Lett. 31 (2020) 2980–2984.
[26] C. Zhang, H. Xie, T. Zhan, et al., Chem. Commun. 55 (2019) 9444–9447.
[27] J. Han, X. Yue, J. Wang, et al., Chin. Chem. Lett. 31 (2020) 1508–1510.
[28] C. Wang, T. Jiang, X. Ma, Chin. Chem. Lett. 31 (2020) 2921–2924.
[29] B. Chen, C. Li, J. Zhang, et al., Chem. Commun. 55 (2019) 7410–7413.
[30] X. Li, J. Zheng, W. Liu, et al., Chin. Chem. Lett. 31 (2020) 2937–2940.
[31] S. Wang, B. Zhou, N. Wang, et al., Chin. Chem. Lett. 31 (2020) 2897–2902.
[32] X.E. Zhao, C. Lei, Y. Gao, et al., Sens. Actuators B: Chem. 253 (2017) 239–246.
[33] S. Liao, X. Zhao, F. Zhu, et al., Talanta 180 (2018) 300–308.
[34] K. Jia, X. He, X. Zhou, et al., Sens. Actuators B: Chem. 257 (2018) 442–450.
[35] H. Lu, C. Yu, S. Xu, Sens. Actuators B: Chem. 288 (2019) 691–698.
[36] G. Ren, Q. Zhang, S. Li, et al., Sens. Actuators B: Chem. 243 (2017) 244–253.
[37] D.K. Dang, S. Chandrasekaran, Y.L. Ngo, et al., Sens. Actuators B: Chem. 255 (2018) 3284–3291.